Journal of Physics: Conference Series **632** (2015) 012001 doi:10.1088/1742-6596/632/1/012001

The knee and beyond: a review of recent results

Andrea Chiavassa

Dipartimento di Fisica dell'Università degli Studi di Torino, Via Pietro Giuria 1, 10125, Torino, Italy

E-mail: andrea.chiavassa@to.infn.it

Abstract. Primary cosmic rays of energy greater than $\sim 10^{14}eV$ must be studied by ground based experiments measuring the particles generated in the EAS (Extensive Air Shower) development in atmosphere. These experiments are mainly limited by the systematic uncertainties on an event due to their energy calibration. I will discuss the main sources of these errors: the choice of the hadronic interaction model and of the mass of the primary particle (that cannot be measured on a event by event basis).

I will then summarize some of the more recent measurements of the all particle spectrum, and I will show that, keeping into account the differences due to the energy calibration, they all agree on the spectral shape. In addition to the well known change of slope, the so called knee, two faint but significant structures have been measured by different experiments: a concavity around $10^{16}eV$ and a steepening at $\sim 10^{17}eV$.

Then I will describe the measurements of the spectra of light and heavy primaries, discussing the claimed spectral features. Using a simple calculation of the elemental spectra (based on the hypothesis that the knee energies follow a Peter's cycle) I will try to discuss if and how these results can be interpreted in a single picture.

1. Introduction

Primary cosmic rays with energy greater than $10^{14}eV$ cannot be studied by experiments operating on balloon or on satellites and their detection is only possible by means of EAS experiments. All the main characteristics of the primary particle (i.e. mass, energy and arrival direction) must therefore be derived measuring the Extensive Air Showers (EAS) generated by the interaction of the primary cosmic rays with atmospheric nuclei.

The experiments operating in the $10^{14} - 10^{18}eV$ energy range can be divided in three groups:

- Surface arrays: sampling the EAS at fixed atmospheric depth. Almost all of these arrays are able to simultaneously detect more than one EAS components: usually the electromagnetic and the muonic ones. Detecting the particle density and arrival times at different distances from the shower core these arrays derive the arrival direction of the primary cosmic ray, the number of charged particles (N_{ch}) and the number of muons (N_{μ}) in the EAS at observation level. Both N_{ch} and N_{μ} are derived as normalization of the lateral distribution of the particle density; either defined as the total number of particles at observation level or as the number of particles at a fixed distance from the shower core (distance that has to be fixed by every single experiment depending both on the detector layout and on the primary energy range studied by the array). These detectors operate with a 100% duty cycle.
- Cherenkov arrays: detecting the Cherenkov light emitted by particles during EAS development. The big advantage of these arrays is that they perform an almost calorimetric

measurement of the primary energy. The atmospheric depth of the EAS maximum (e.g. a shower parameter depending on the mass of the primary particle) can be estimated comparing the Cherenkov photon densities measured at two different distances from the shower core. These arrays operate only during clear moonless nights, thus their duty cycle is $\sim 10 - 15\%$.

- Fluorescence light telescopes: if the primary energy is greater than $\sim 5 \times 10^{16} eV$ EAS can also be detected measuring the fluorescence light emitted during their development. The major advantage of these detectors is that they allow a calorimetric determination of the primary energy and therefore their calibration does not rely on EAS simulation. The experimental observable sensible to the primary mass is the atmospheric depth of shower maximum. Like Cherenkov arrays also these detectors operate with a low duty cycle.

The main problem of these experiments is that energy, excluding fluorescence telescopes, and mass calibrations have to be performed by means of EAS simulations that are based on hadronic interaction models extrapolated from lower energy collider measurements. Recently the results coming from the LHC experiments [1] are filling this gap, nevertheless collider experiments do not cover the forward region that is the relevant one to describe the EAS development.

In spite of all the mentioned calibration problems the results of last generation experiments allowed a deeper understanding of the knee of the primary cosmic ray spectrum, the major achievements are:

- the detection, in addition to the main feature of the spectrum (i.e. the knee, at $\sim 2-4\times10^{15} eV$ [2]), of two faint structures, an hardening around $10^{16} eV$ and a steepening around $10^{17} eV$ [3, 4, 5].
- The measurement of the spectra of light and heavy primaries [6, 7, 8, 9]. The spectral features observed in these spectra slightly depend on the hadronic interaction model on which the energy and mass calibration of the experiments are based, while the same is not true for the measured fluxes.
- By unfolding analysis techniques the spectra of five elements (chosen as representative of five mass groups) have been measured [10, 11]. These results heavily depend on the hadronic interaction model used in the EAS simulation, therefore I will briefly mention them but I will not use them in the final discussion.
- The measurement of a large scale anisotropy at $2 \times 10^{15} eV$ [12]. The phase of the first harmonic is compatible with the ones measured at $\sim 4\times10^{14} eV$ [13, 14], while the amplitude is increasing.

The scenario resulting from such measurements favors an astrophysical interpretation of the knee, even if the resulting picture is not complete and, to further improve our knowledge, high precision experimental results are needed. I will show that recent results can, at least qualitatively, be described by elemental spectra having the change of slope at energies depending on Z, even if the recent ARGO-YBJ results [9] cannot be easily included in such a simple framework. Moreover in order to accurately describe the structures observed above the knee, an additional component must be introduced [15, 16].

In this review I discuss some of the more recent experimental results, while no description of the models proposed to discuss them is given. A final discussion showing the results of a simple calculation of the primary spectra and only aiming to a qualitative interpretation of the data is reported.

2. Energy and Mass Calibration of Ground Based Experiments

2.1. Energy Calibration

Surface arrays derive the energy of the primary particle either from the measured value of the number of charged particles (N_{ch}) either from the measured value of the number of muons (N_μ)

or from a combination of both.

All these shower parameters depend not only on the energy of the primary cosmic ray but also on the atmospheric depth crossed by the EAS, thus also the zenith angle θ has to be taken into account. The shower evolution in atmosphere can be treated in two different ways: a first one is based on the experimental data supposing that the arrival directions of cosmic rays are isotropically distributed, the so called "constant intensity cut" technique [17], while a second one describes the EAS atmospheric evolution by means of their simulation.

The main sources of systematic errors in the energy calibration of any EAS experiment are related to the use of a complete EAS simulation and are therefore connected to the two main hypotheses that must be done when running these codes: the mass of the primary particle generating the shower and the hadronic interaction model describing high energy interactions.

Considering the choice of the mass of the primary particle three different strategies are possible:

- the primary energy is calculated for the two extreme values of the primary mass (Hydrogen and Iron). The spectra that are obtained for these two cases represent the upper and lower limits bracketing the "true" spectrum (an example can be found in [18]).
- Starting from the primary chemical composition measured at lower energy by direct experiments and assuming its evolution with energy the mean value of the primary mass is calculated as a function of the primary energy (an example can be found in [4]). This mean value of the primary mass is then used to convert the experimental observable to primary energy.
- Combining the N_{ch} and N_{μ} values measured for each event a parameter correlated with the mass of the primary particle is evaluated. Then this parameter is used in the conversion from the experimental observable to the primary energy [3]. In this way no assumption is made about the primary chemical composition, but a further dependence on the hadronic interaction model is added (in the definition of the parameter correlated with the primary mass).

Cherenkov experiments derive the primary energy from the photon density measured at a fixed distance from the shower core, $200m$ in the case of the TUNKA-133 experiment [5]. Considering TUNKA-133 as reference experiment the correlation between $Q(200)$ and the primary energy is given by:$E_0 = CQ(200)^g$. The parameter g is evaluated by mean of the CORSIKA [19] simulation code, $g = 0.94 \pm 0.01$. The value of the constant C is obtained normalizing the integral energy spectrum of each single night of data taking to a reference one measured by the QUEST experiment[20].

The second main source of systematic error in the energy calibration of EAS experiments is the choice of the hadronic interaction model in the EAS simulation. The center of mass energy of the interaction between an high energy cosmic ray and an air nuclei is well above the ones studied at collider experiments. The reference hadronic interaction models used by current EAS experiments are: QGSJetII-02 [21], Sibyll2.1 [22] and EPOS1.99 [23]. The KASCADE-Grande experiment has evaluated the differences in the energy assignment due to the hadronic interaction model choice [24], finding that they are smaller than 20% and with a slight energy dependence. The all particle spectra derived from the KASCADE-Grande data calibrated by means of these three different hadronic interaction models are shown in figure 1.

Recently updates of two of the three previously mentioned hadronic interaction models based on the results obtained by LHC experiments have been included in the CORSIKA EAS simulation code: QGSJetII-04 [25] and EPOS-LHC [26]. First studies performed by the KASCADE-Grande collaboration [27] indicate that the differences between the energy calibrations obtained using hadronic interaction models developed before (QGSJetII-02, Sibyll2.1 and EPOS1.99) and after (QGSJetII-04 and EPOS-LHC) the LHC data are smaller than 20%.

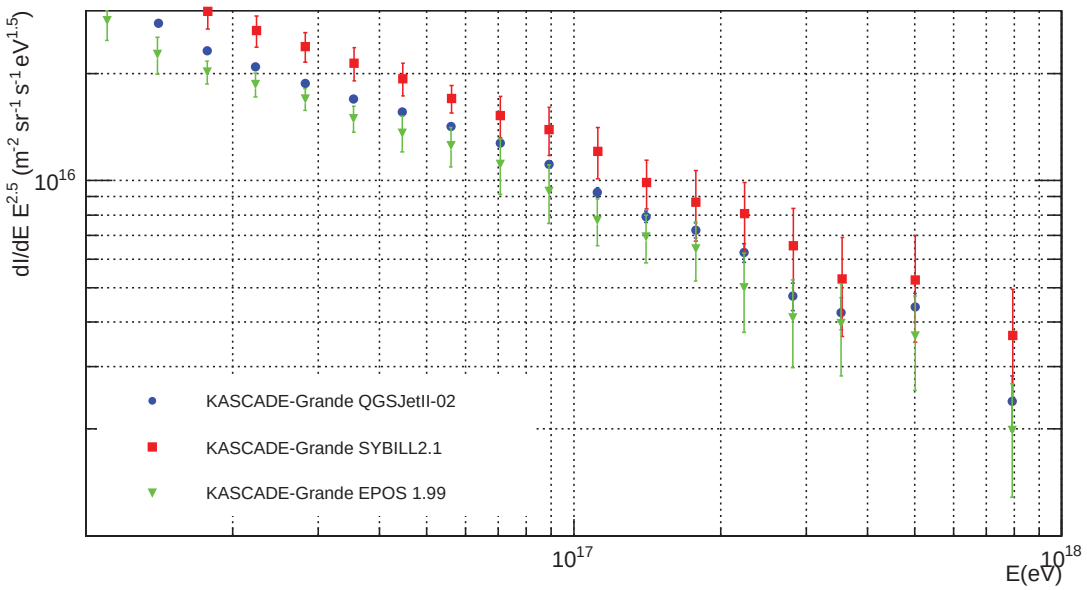

Figure 1. KASCADE-Grande measurements of the all particle energy spectra calibrated by mean of three different hadronic interaction models: QGSJetII-02, Sibyll2.1 and EPOS1.99

2.2. Mass Calibration

Due to the intrinsic fluctuations in the EAS development ground based experiments cannot access the mass of every single event. Even at shower maximum (where the fluctuations are minimized) the differences between EAS generated by primaries of similar mass (i.e. H and He, He and CNO, Si and Fe) are smaller than one standard deviation. Studies of the primary chemical composition can be performed using statistical methods like, for instance, the unfolding analysis introduced by the KASCADE experiment [10, 11], or separating events in two mass groups, i.e. light and heavy primaries.

The shower observables sizable to such purpose are:

- the measurement of the shower maximum development. With current detection techniques this information can be directly obtained only by fluorescence light telescopes, while Cherenkov detectors can infer it either from the ratio of the photon densities at two different distances from the shower core and from the measurement of the pulse width at 400 m from the core [5].
- The ratio between observables representing the charged particle and the muon numbers at observation level.
- A correlation between a parameter proportional to the number of particles at observation level and another one reflecting the shape of the particle lateral distribution.

In order to assign a value of the primary mass to any of the previously indicated experimental observables a complete EAS simulation is needed, therefore these analyses depend on the high energy hadronic interaction model.

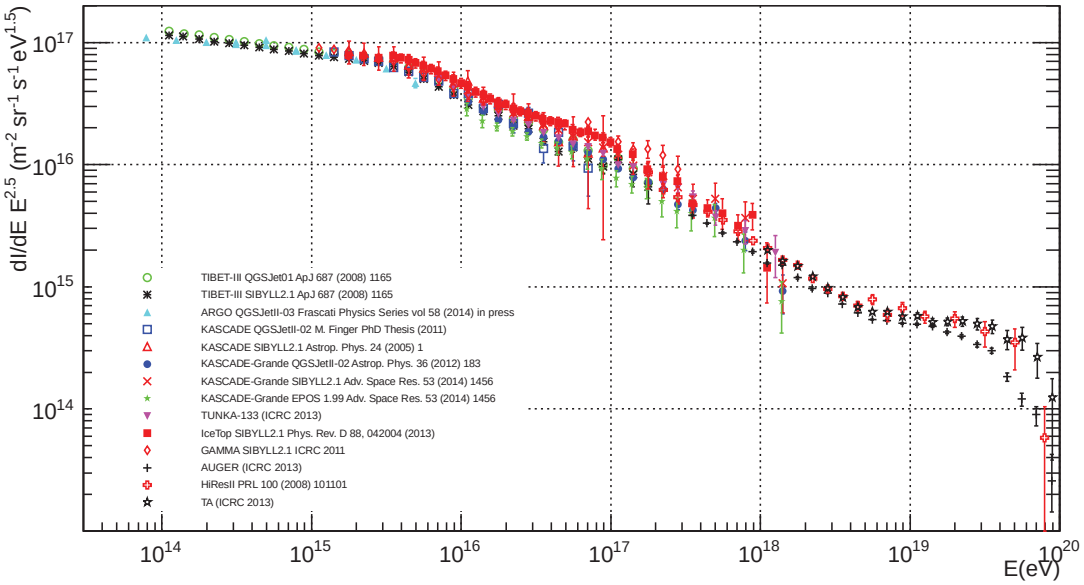

Figure 2. Compilation of all particle energy spectra measurements[28, 9, 29, 10, 3, 24, 5, 4, 30, 31, 32, 33]

3. Experimental Results

Having discussed the main sources of systematic uncertainties affecting the energy and mass measurements performed by EAS experiments, in this section I will discuss some of the more recent results obtained in the $10^{14} - 10^{18} eV$ energy range.

3.1. All Particle Energy Spectrum Measurements

Figure 2 shows a compilation of the all particle energy spectrum measured by different experiments using different experimental techniques, operating at different height above see level and calibrated by different hadronic interaction models. From this plot we can get the impression of measurements showing relevant differences between each other, but simply shifting, as already proposed in [16], the single experiment energies by an amount lower than the previously discussed systematic uncertainties (i.e. $\Delta E/E \leq 20\%$) all these results agree much better, as can be seen in figure 3. The differences shown in figure 2 can thus be attributed to the energy calibration of the experiments. There is a general agreement about the cosmic rays spectrum in the $10^{14} - 10^{17} eV$ energy range that cannot be described by a single slope power law showing three features: the well known steepening observed by Khristiansen et al. [2] more than fifty years ago at $2 - 4 \times 10^{15} eV$ (better known as the knee); a concavity at $\sim 10^{16} eV$ and a faint steepening around $\sim 10^{17} eV$ first claimed by KASCADE-Grande [3] and then confirmed by IceTop [4] and TUNKA-133 [5].

3.2. Mass Groups Energy Spectra

Ground based experiments can measure the spectra of mass groups of primary cosmic rays by two different approaches that will be described in the following.

A first analysis technique separates the events in two samples according to the measured ratio

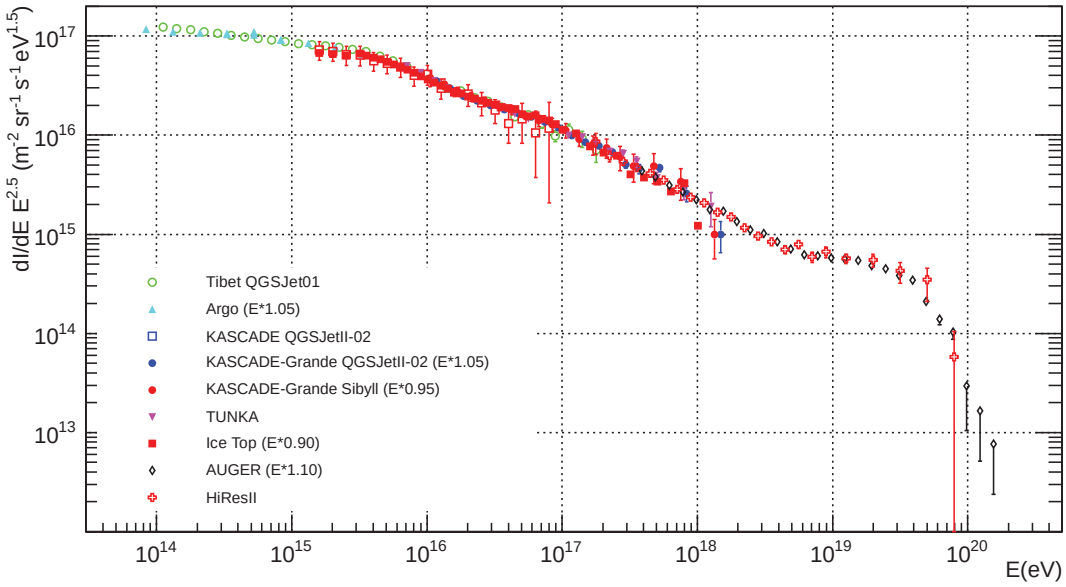

Figure 3. All particle energy spectrum measured in the $10^{14} - 10^{20} eV$ energy range. The energy calibration of the experiments are shifted by an arbitrary amount smaller than the systematic errors. References can be found in the caption of figure 2 and the energy shifts applied are indicated in the legend inside the plot.

between the muon and charged particles numbers, converted, by means of the constant intensity cut, to a reference zenith angle. The events sample with a high value of this parameter (called Y by the KASCADE collaboration who introduced this analysis technique [6]) is generated by heavy primaries and the one with low Y values by the light ones. The KASCADE-Grande experiment has then slightly modified this analysis [7, 8] calculating the ratio between muon and charged particles numbers in small intervals of zenith angles (i.e. atmospheric depth).

A similar approach has been used by the ARGO-YBJ collaboration [9] that, being a full coverage detector operating at higher altitude (i.e. almost near to shower maximum) and not having a muon detector, selected the events on the basis of the ratio between the number of particles measured within a distance of $8m$ from the shower core (Np_8) and the slope (s') of the lateral distribution function.

In both techniques a selection level must be determined to divide the two samples, this cut has to be defined according to the results of a complete EAS simulation. In the case of the KASCADE and KASCADE-Grande experiments it was shown that the level used to define the two samples affects only the absolute fluxes of the spectra, while eventual spectral features are visible independently from this choice that only enhances them. Defining the hadronic interaction model the choice of the cut value corresponds to a primary mass, while at constant primary mass defining a cut value means selecting simulations performed with a particular hadronic interaction model. Thus a spectral feature measured independently from the cut value does not depend on the hadronic interaction model used in the EAS simulation.

Figure 4 shows a summary of the, energy calibrated, KASCADE-Grande and ARGO-YBJ measurements of the light primaries spectra. In the plot also the direct measurements of the H and He spectra performed by the CREAM collaboration [38] are shown, their agreement with

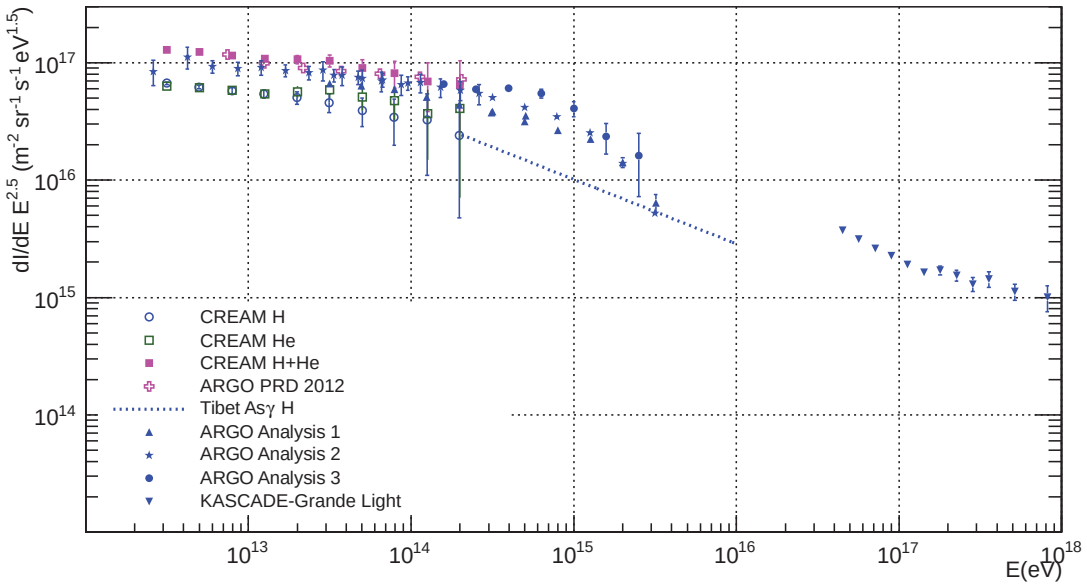

Figure 4. Spectra of the light primaries measured by ARGO-YBJ (the different analysis shown by the collaboration are described in [9]) and KASCADE-Grande. Lower energy direct measurements of the CREAM experiment are shown as a reference. The former KASCADE measurements are not shown in this plot as the light primaries spectrum was shown in a non energy calibrated way [6]

the low energies measurement of the ARGO-YBJ experiments confirms the validity of the energy calibration of this experiment and suggests also the good reliability (at least around $10^{13}eV$) of the hadronic interaction models included in the CORSIKA code.

The KASCADE experiment published [6] the spectra of the "electron rich" (i.e. light primaries) and the "electron poor" (i.e. heavy primaries) events. These spectra are not calibrated in energy (they are shown as a function of the muon density at fixed core distance), but using the integral flux above the change of slope we can identify this feature with the knee of the all particle energy spectrum.

The ARGO-YBJ collaboration has shown [9] the results of three different analysis differing between each other by an amount lower than the declared systematic errors, all the three spectra show a break well below $10^{15}eV$. But, in my opinion at the moment of writing this contribution, some details of these results are doubtful:

- different spectra have different slopes, mainly above the break.
- The spectrum of the light elements changes slope at an energy different from the one where the all particle spectrum changes its slope. It seems strange that, being the light elements a fraction near to the 50% of the cosmic rays flux, such a sharp change of slope is not visible in the all particle spectrum.

On another hand this claim is in agreement with the one of the Tibet-ASγ collaboration who measured the hydrogen spectrum above $\sim 10^{14}eV$ and found a spectrum steeper than the one detected below the knee [39]. The Tibet-ASγ collaboration concluded that the hydrogen knee is

at lower energy and that the change of slope in the all particle spectrum observed at $2-4\times10^{15}eV$ is due to heavy elements.

The KASCADE-Grande experiment published the spectra of the light and heavy components in two slightly different energy ranges with selection cuts differently defined in order to enhance their spectral features:

- an hardening of the light component spectrum [8]: at $10^{17.08\pm0.08}eV$ the spectral slope changes from $\gamma = -3.25 \pm 0.05$ to $\gamma = -2.79 \pm 0.08$.
- A steepening of the heavy primaries spectrum [7]: at $log(E/eV) = 16.92 \pm 0.04$ the spectral slope γ changes from $\gamma = -2.76 \pm 0.02$ to $\gamma = -3.24 \pm 0.05$.

A different approach to derive the spectra of single elements (representative of different mass groups) is the one based on the unfolding analysis technique. The goal of this analysis, introduced by the KASCADE experiment [10], is to obtain the elemental fluxes from the bi-dimensional spectra N_e *vs* N_μ. The number of events measured in each pixel of this spectrum are compared with the one expected by a complete EAS and detector simulation. This approach allows to take into account the EAS development fluctuations and the reconstruction errors, but the results heavily depend on the hadronic interaction model used in the EAS simulation. The KASCADE collaboration reported results based on different hadronic interaction model presenting differences in the fluxes of the elemental spectra, but revealing common features: only the spectra of light elements show a change of slope and the knee energy increases with the primary atomic number.

Elemental spectra in agreement with the ones previously discussed have been obtained, at greater energies, by the KASCADE-Grande collaboration using the same unfolding algorithm [11]. The iron spectrum shows a hint of a steepening at an energy in agreement with the one where the knee of the heavy elements has been observed.

3.3. Large Scale Anisotropy

In the $10^{14}-10^{16}eV$ energy range the expected anisotropies are of the order of $10^{-3}-10^{-4}$, while the variation of the number of counts induced by atmospheric (i.e. pressure or temperature) and instrumental effects are greater by at least one order of magnitude. It is thus clear that these fake anisotropies must be removed in order to enhance the real ones. The IceCube and IceTop experiments have applied the time-scrambling algorithm [34] while KASCADE-Grande used the East-West analysis technique [35]. The experimental sensitivity in the search for large scale anisotropies of the cosmic rays arrival distribution is mainly limited by the number of events accumulated by the experiments, being the error on the amplitude proportional to $\sqrt{N_{events}}$.

Statistically significant detection of large scale anisotropies in the $10^{13}-5\times10^{16}eV$ have been obtained by EAS-TOP [14] at $100TeV$ and $400TeV$, IceCube [13] at $20TeV$ and $400TeV$ and IceTop [12] at $400TeV$ and $2PeV$. At greater energies have been published only the upper limits obtained by the KASCADE [36] and KASCADE-Grande [37] experiments. The amplitudes of the first harmonic are shown in figure 5, while the relative phases can be seen in figure 6. We can notice that there is a trend of an increasing amplitude above $10^{14}eV$ and that, at the same energy, the phase is changing (as confirmed also by KASCADE-Grande). Even if we must consider that the IceTop results cannot be well described by the sum of a dipole and a quadrupole thus an harmonic description of the anisotropy maybe a simplified one.

4. Discussion

In this section I present the results of a calculation, based on the work of T. Gaisser et al. [16], of elemental spectra following a Peter's cycle (i.e. with knee energies at constant rigidity). My goal is neither reaching a detailed interpretation of the data nor making any fit to obtain the

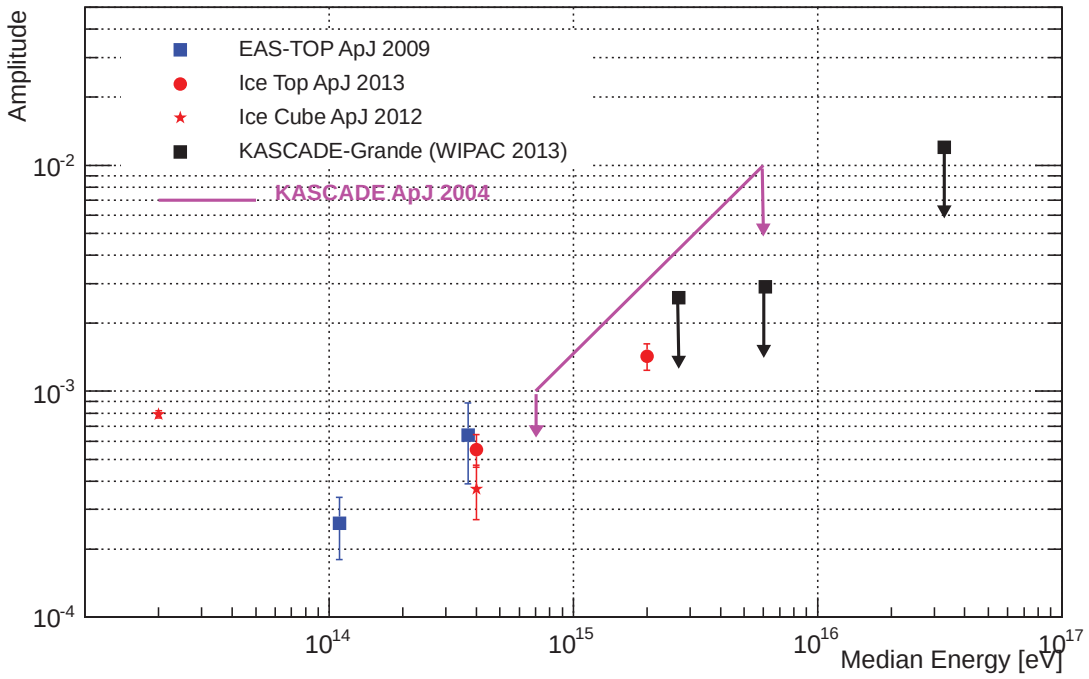

Figure 5. Amplitudes of the first harmonic measured in the $10^{13} - 5 \times 10^{16} eV$ energy range. The results of the EAS-TOP, IceTop and IceCube experiments are measurement of the first harmonic amplitude, while the KASCADE and KASCADE-Grande ones are upper limits.

elemental spectra describing them, I will only search for a qualitative agreement between the data shown in section 3 and the calculated spectra.

The elemental spectra are calculated with an expression [40] describing a power law with index changing from γ_1 to γ_2 at an energy E_{knee}.

$$\Phi(E) = KE^{\gamma_1}[1 + (\frac{E}{E_{knee}})^{\epsilon}]^{\frac{(\gamma_2-\gamma_1)}{\epsilon}} \quad (1)$$

The parameter ϵ represent the sharpness of the change of slope, and in these calculations has been kept constant ($\epsilon = 10$) corresponding to a smooth knee.

The elemental fluxes have been calculated with the following hypotheses:

1) the absolute normalization is given by the intensities measured by CREAM [38] at $10^{13} eV$.
2) The slopes of the H and He spectra before the knee are the ones measured by CREAM, the slope of the He spectrum is used also for heavier elements.
3) All the spectra suffer the same change of slope, values ranging from $\Delta\gamma = 0.5$ to $\Delta\gamma = 0.7$ have been used.
4) The knee energy has been calculated following a Peter's cycle: $E_{knee}(Z) = Z \times E_{knee}(H)$. The Hydrogen knee is fixed at two different energies: $E_{knee}(H) = 6.5 \times 10^{14} eV$ following the ARGO-YBJ results and $E_{knee}(H) = 1.5 \times 10^{15} eV$ attributing the knee of the all particle spectrum to a light element, i.e. either H or He.

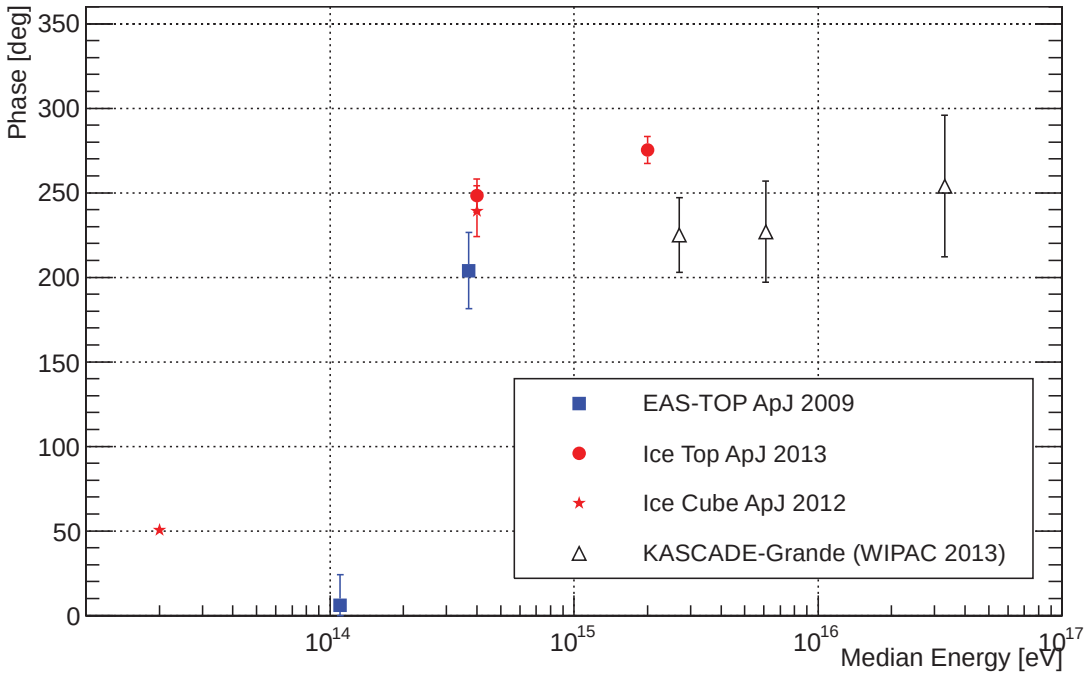

Figure 6. Phases of the first harmonic measured in the $10^{13} - 5 \times 10^{16} eV$ energy range

.

5) To account for the hardening of the light elements spectrum a flatter H component ($\gamma = -2.66$) becoming dominant at $\sim 10^{17} eV$ is added.

This is only one of the possible options to calculate the elemental spectra of cosmic rays, for instance one can assume different slopes for all the elements heavier than Helium or that the knee energies depends on the mass of the primaries (and not on their charge).

Comparing the results of these calculations with the mass group spectra we must always keep in mind that the intensities measured with these algorithms aim to enhance spectral feature and not to determine the absolute fluxes. To better show this qualitative agreement I multiply the calculated spectra by a factor that can be interpreted as the selection efficiency of events generated by a particular primary element. The goal of this factor is not to evaluate these efficiencies but it must be intended as an help to guide the eyes in evaluating this qualitative agreement.

In figure 7 the ARGO-YBJ light and all particle spectra are shown together with the results of the previously described calculations. We can see as the sharp knee of the light elements spectrum can be described fixing a huge value for the change of slope ($\Delta\gamma = 0.7$), but summing all elements to calculate the all particle spectrum we cannot describe the Tibet-III [28] and ARGO-YBJ measurements. This disagreement can be reduced assuming that the knee energy depends on the mass of the primaries (A) or using harder spectra for elements heavier than He, but it is in any case difficult to obtain a good description of both the light and the all particle spectra. If these results will be confirmed an additional (heavy?) component must be invoked.

Extending the elemental spectra calculations from $10^{14} eV$ to $5 \times 10^{18} eV$ we can compare the

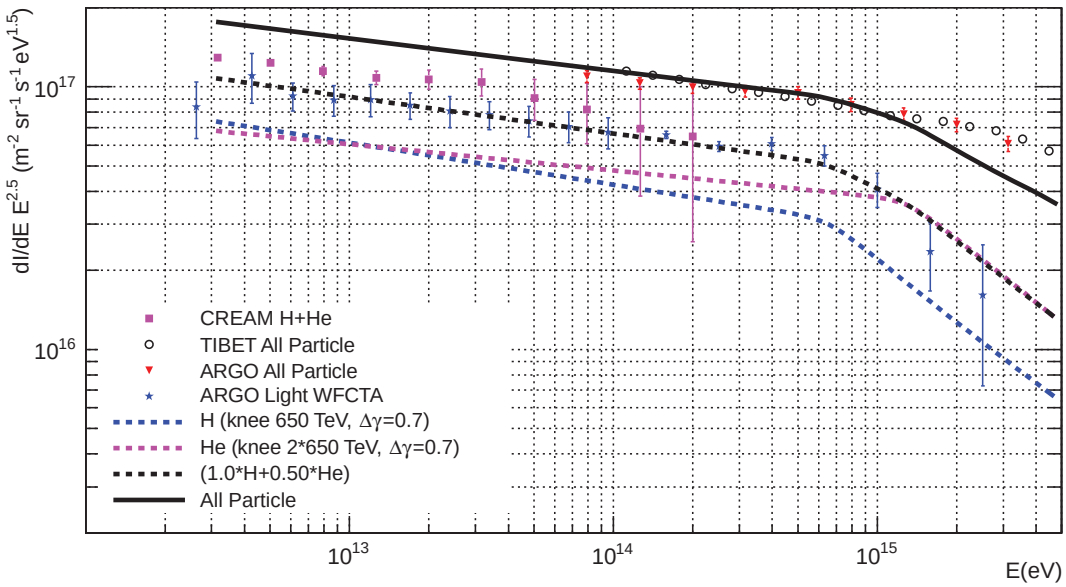

Figure 7. All particle and light elements spectra measured by the ARGO-YBJ experiment compared with the calculations described in section 4

.

expectations with the measurements in a wide energy range, in figure 8 I show the calculated fluxes and the experimental data (with the energy shifted by an arbitrary factor, see figure 3). Thus in addition to the simplified and schematic approach there is also an uncertainty about the absolute fluxes, therefore we can only expect a qualitative agreement between data and calculations. The shown fluxes correspond to: H (blue solid line), He (magenta dashed line), C (red dotted line), Fe (green dash-dotted line) and their sum (black thick solid line).

We can see that the knee structure is well reproduced by elemental spectra following Peter's cycle, but further details must be clarified by future experiments, such as:

- which element is dominating the spectrum at the knee?
- If all the claimed results are confirmed, is there a contradiction between measurements performed at high altitudes and at sea level?
- Which is the exact energy of the knee?
- The knee energies of different elements depend on their charge (Z) or their mass (A)?
- At energies smaller than the knee are the spectral indexes of all elements (except H) equal or not?
- Is the change of slope at the knee the same for all elements?

Figure 8 shows also that at energies above the knee such a simple calculation cannot explain the faint structures measured at $\sim 10^{16} eV$ and $\sim 10^{17} eV$, therefore (as already pointed out by T. Gaisser et al. [16]) an additional galactic component, such as the "component B" proposed by Hillas [15], is needed to explain the measured fluxes. The contribution of an additional (extra-galactic?) H flux becoming dominant at $\sim 10^{17} eV$ can, qualitatively, describe the hardening of the light elements spectrum measured by KASCADE-Grande.

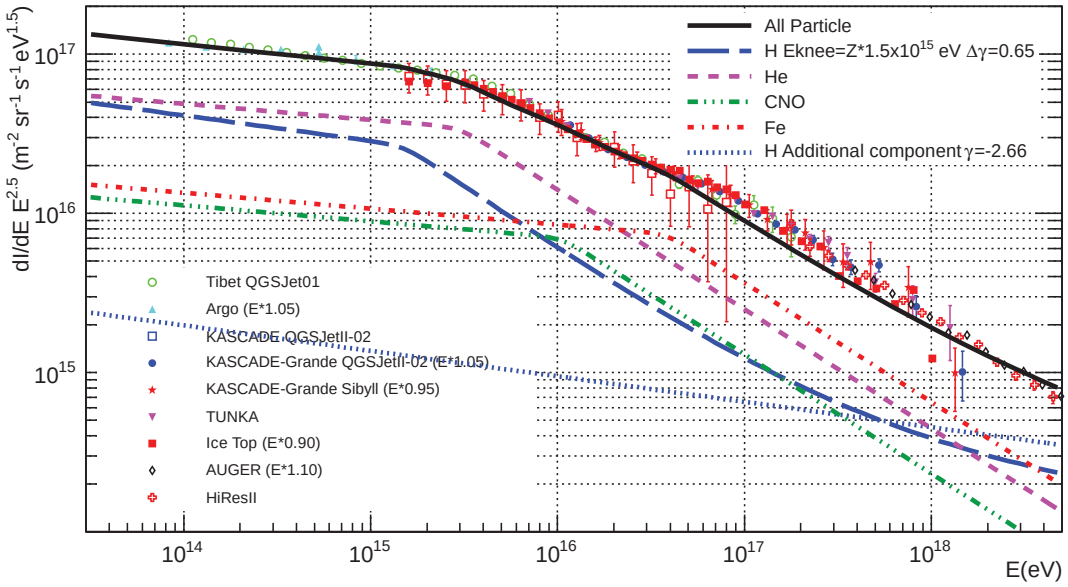

Figure 8. Summary of all particle spectrum measurements, shifted by an arbitrary amount (reported in the legend), and compared with the calculations described in section 4

.

Thus new, high precision measurements are required. These can be performed either by direct, high acceptance measurements or by high resolutions EAS arrays. Both techniques have their advantages and limitations:

- Direct measurements. Long duration satellite experiments, like the foreseen iss-cream [41], will be able to collect enough statistics to cover the knee energy and will have the charge resolution to separate single elements. Their main limitation will be the low energy resolution ($\sim \Delta E/E \sim 40\%$) due to the strong constrain on their mass. Calorimetric detectors will contain only a small fraction of the shower generated the primary particle interaction. Furthermore no man made sources will be available at these energies, thus the absolute energy calibration will be performed indirectly by simulations.
- EAS measurements. The main limitation of ground based experiments will always be the EAS development fluctuations. The best way to minimize them is to locate the array at high altitudes in order to detect the showers near their maximum development. This is the goal of the LHAASO experiment [42] that will be constructed in China, Sichuan province at $\sim 4400m$ *a.s.l.*. This experiment will sample the electromagnetic and muonic shower components with an unprecedented active surface and will therefore reach an unprecedented resolution.

References

[1] T. Pierog, EPJ Web of Conferences **52**, 03001 (2013).
[2] G.V. Kulikov,G.B. Khristiansen, Sov. Phys. JEPT **35**, 441 (1958).
[3] W.D. Apel et al., Astropart. Phys. **36**, 183 (2012).
[4] M.G. Aartsen et al., Phys. Rev. D **88**, 042004 (2013).
[5] V.V. Prosin et al., Nucl. Instr. and Meth. A **756**, 94 (2014).

[6] T. Antoni et al., Astropart. Phys. **16**, 373 (2002).
[7] W.D. Apel et al., Phys. Rev. Lett. **107**, 171104 (2011).
[8] W.D. Apel et al., Phys. Rev. D **87**, 081101(R) (2013)
[9] G. Di Sciascio on behalf of the ARGO collaboration, Frascati Physics Series **58**, (2014) in press
[10] T. Antoni et al., Astropart. Phys. **24**, 1 (2005).
[11] W.D. Apel et al., Astropart. Phys. **47**, 54 (2013).
[12] M.G. Aartsen et al., ApJ **765**, 55 (2013).
[13] R. Abbasi et al., ApJ **746**, 33 (2012).
[14] M. Aglietta et al., ApJ **692**, L130 (2009).
[15] A.M. Hillas, J. Phys. G: Nucl. Part. Phys. **31**, (2005) R95.
[16] T.K. Gaisser et al., Front. Phys. **8(6)**, 748 (2013).
[17] J. Hersil et al., Phys. Rev. Lett., **6**, 22 (1961); D.M. Edge et al., J. Phys. A, **6**, 1612 (1973).
[18] D. Kang et al., Proc. of the 31^{st} ICRC Lodz (Poland), #icrc1044 (2009).
[19] D. Heck et al., Report FZKA 6019, Forschungszentrum Karlsruhe (1998).
[20] E.E. Korosteleva et al., Nucl. Phys. B (Proc. Suppl.) **165**, 6837 (2007).
[21] S. Ostapchenko, Phys. Rev. D **74**, 014026 (2006).
[22] E.-J. Ahn et al., Phys. Rev. D **80**, 094003 (2009).
[23] K. Werner, F.M. Liu, T. Pierog, Phys. Rev. C **74**, 044902 (2006).
[24] W.D. Apel et al., Advances in Space Research **53**, 1456 (2014).
[25] S. Ostapchenko, Phys. Rev. D **83**, 014018 (2011).
[26] T. Pierog et al., arXiv:1306.0121, (2013).
[27] M. Bertaina et al., Nucl. Phys. B (Proc. Suppl.) **256-257**, 149 (2014).
[28] M. Amenomori et al., ApJ **678**, 1165 (2008).
[29] M. Finger, PhD Thesis, Karlsruhe University (2011)
[30] A.P. Garkaya et al., J. Phys. G: Nucl. Part. Phys. **35**, 115201 (2008).
[31] A. Aab et al., arXiv:13075059v1, (2013).
[32] R.U. Abbasi et al., Phys. Rev. Lett. **100**, 101101 (2008).
[33] T. Abu-Zayyad et al., arXiv:1305:7273, (2013).
[34] D.E. Alexandreas et al., Nucl. Instr. and Meth. A **328** , 570 (1993).
[35] R. Bonino et al., ApJ **738**, 67 (2011).
[36] T. Antoni et al., ApJ **604**, 687 (2004).
[37] A. Chiavassa et al., Jour. of Phys. Conf. Series **531**, 012001 (2014).
[38] Y.S. Yoon et al., ApJ **728**, 122 (2011).
[39] M. Amenomori et al., Physics Letters B **623**, 58 (2006).
[40] S.V. Ter-Antonyan and L. Haroyan, arXiv:hep-ex/0003006, (2000).
[41] E.S. Seo et al., Proc. of the 33rd ICRC (Rio de Janeiro, Brasil), #0629 (2013).
[42] Cao Z., Chinese Physics C **34**, 249 (2010).